Published in final edited form as:
Cell. 2009 January 9; 136(1): 163–174. doi:10.1016/j.cell.2008.11.046.

The Mechanism of Kinesin Regulation by Ca^{++} for Control of Mitochondrial Motility

Xinnan Wang and **Thomas L. Schwarz***
F. M. Kirby Neurobiology Center, Children's Hospital Boston, and Department of Neurobiology, Harvard Medical School, Boston, MA 02115, USA.

SUMMARY

Cells regulate mitochondrial movement in order to distribute mitochondria properly and thereby meet the changing energy needs of each region of the cell. Ca^{++} signaling, which halts both anterograde and retrograde mitochondrial motion, is one such regulation. We show that the EF-hands of Miro mediate this arrest and elucidate the regulatory mechanism of the motor kinesin-1. Kinesin-1 remains on mitochondria whether they are stationary, moving anterograde, or moving retrograde and the protein complex that couples kinesin-1 to mitochondria is not dissociated by elevated Ca^{++}. Instead, Ca^{++}-binding to Miro permits Miro to interact directly with the motor domain, thereby preventing motor/microtubule interactions. This switching mechanism allows Ca^{++} to regulate mitochondrial motility via two kinesin states: an active state in which kinesin is bound to mitochondria via its tail and milton, and an inactive state in which the motor domain binds directly Miro. Disrupting this regulation diminishes neuronal resistance to excitotoxicity.

INTRODUCTION

Molecular motors are responsible for distributing proteins and organelles within the cell. To achieve the correct spatial distribution of these cargos, and to change that distribution in response to changing conditions, these motors need to be precisely regulated. Although great progress has been made in identifying molecular motors and studying the biophysical mechanisms of their movement, much less is known about how these motors are regulated (Gross et al., 2007). The dynamic regulation of motors is especially important for mitochondria, which are frequently in motion. Particularly in neurons, whose highly extended processes are highly dependent on organelle transport, regulation of motors permits mitochondria to redistribute themselves to balance the changing energy needs of each portion of the cell (Hollenbeck and Saxton, 2005).

All cells depend on mitochondria for local ATP supply and Ca^{++} buffering. In neuronal axons and dendrites these requirements need to be addressed locally and not by diffusion from distant cell bodies. Consequently, defects in mitochondrial distribution can underlie neurodegenerative disease (Chen and Chan, 2006; Petrozzi et al., 2007). Moreover, because the demand for energy and the need for Ca^{++} buffering differ from one neuron to another and indeed from one part of the neuron to another part, the density of mitochondria differs between

*Correspondence: thomas.schwarz@childrens.harvard.edu.

neurons and within a single neuron. The task of distributing mitochondria properly in a neuron to balance changing energy needs may therefore require particularly dynamic regulation.

Reflecting the dynamic nature of these organelles, many axonal mitochondria are in motion, traveling both long and short distances and starting and stopping often (Chang et al., 2006; Hollenbeck and Saxton, 2005; Overly et al., 1996). The majority of these movements are microtubule-based, either anterograde, toward the (+)-ends of the microtubules in the periphery, or retrograde, toward the (-)-ends in the cell bodies. The behavior of mitochondria is therefore primarily governed by the interplay of (+)-end directed kinesin motors, the (-)-end directed dynein motor, and tethering proteins that may hold mitochondria in place (Chada and Hollenbeck, 2003, 2004; Hollenbeck and Saxton, 2005; Kang et al., 2008; Morris and Hollenbeck, 1995). How multiple motors on an organelle are coordinated is not yet understood.

Kinesin-1, the conventional kinesin whose motor domain resides in kinesin heavy chain (KHC), appears to be the primary anterograde motor for mitochondria (Glater et al., 2006; Hurd and Saxton, 1996; Pilling et al., 2006; Tanaka et al., 1998). We previously demonstrated the existence of a motor/adaptor complex containing KHC and two proteins, milton and Miro, that are also essential for the axonal transport of mitochondria (Figure 1A) (Glater et al., 2006; Stowers et al., 2002). KHC is recruited to mitochondria by binding to milton, which in turn binds to the cytoplasmic surface of the mitochondrion by interacting with Miro, a transmembrane protein of the outer-mitochondrial membrane (Fransson et al., 2003; Fransson et al., 2006; Glater et al., 2006; Guo et al., 2005). This complex is conserved from flies to mammals (Beck et al., 2002; Brickley et al., 2005; Fransson et al., 2003; Glater et al., 2006; Stowers et al., 2002) and is likely to govern aspects of mitochondrial distribution in many cell types, including neurons (Glater et al., 2006; Guo et al., 2005; Stowers et al., 2002), oocytes (Cox and Spradling, 2006) and muscle (Guo et al., 2005). In yeast, a homolog of Miro (GEM1p) also influences mitochondrial distribution (Frederick et al., 2004). A regulatory role is indicated for Miro by its Ca^{++}-binding sites and Rho-like GTPase domains and for milton by its post-translational modifications and splicing variants.

Several intracellular signals have been shown to control the movement of mitochondria and thereby influence mitochondrial distribution (Boldogh and Pon, 2007; Chada and Hollenbeck, 2003, 2004; Kang et al., 2008). The most widely studied of these is intracellular Ca^{++} which, when elevated, arrests microtubule-based mitochondrial movement in many cell types (Chang et al., 2006; Hollenbeck and Saxton, 2005; Rintoul et al., 2003; Szabadkai et al., 2006; Yi et al., 2004), although the bulk of fast axonal transport persists in the presence of Ca^{++} (Brady et al., 1984). Ca^{++} influx occurs in regions of high metabolic demand, such as nerve terminals and postsynaptic specializations where the extrusion of ions is energetically expensive and where mitochondria are concentrated. In addition, sustained elevated cytosolic Ca^{++} may be a symptom of insufficient local ATP to power Ca^{++} export across the plasma membrane, or impaired buffering capacity of mitochondria due to decreased activity of the electron transport chain. Thus a tendency for mitochondria to arrest where Ca^{++} is elevated will cause them to be retained where energy requirements are high and supplies are low and will thereby balance ATP production to local need. How Ca^{++} halts mitochondrial motility is presently unknown.

Because Miro contains a pair of EF-hand Ca^{++}-binding motifs, we hypothesized that the KHC/milton/Miro complex would mediate the Ca^{++}-dependent regulation of mitochondrial motility. By examining mitochondrial movement in transfected neurons, we here show that the EF-hands are essential for this regulation and elucidate the mechanism of kinesin inhibition.

RESULTS

Milton Recruits KHC to Neuronal Mitochondria

Previous work from this lab and others has established that milton, Miro, and KHC, whether from *Drosophila* or mammals, coprecipitate when expressed in cell lines (Beck et al., 2002; Brickley et al., 2005; Fransson et al., 2003; Glater et al., 2006; Stowers et al., 2002). Endogenous mammalian KHC, milton and Miro also coprecipitated as a complex from HEK293T cells (Figure 1B). Furthermore, in transfected COS cells, overexpressed KHC will be recruited onto mitochondria only if milton is co-expressed and that milton binding to mitochondria is mediated by Miro (Glater et al., 2006), supporting the model in Figure 1A. Because *milton* and *Miro* mutations prevent anterograde transport of mitochondria in *Drosophila* axons and because milton and KHC co-precipitate from *Drosophila* head extracts, we have presumed that the same complex mediated the mitochondrial association of KHC in neurons. To test this hypothesis, we have transfected rat hippocampal neurons with a fluorescently tagged KHC (KHC-mCit), Miro-Myc, and an RFP tagged mitochondrial-import sequence (RFP-mito) (Colwill et al., 2006; Fransson et al., 2006; Cai et al., 2007), in the presence or absence of co-transfected milton. The specificity of RFP-mito as a mitochondrial marker in these cultures was ascertained by costaining with a mitochondrial dye and antibodies to the mitochondrial protein Miro (Figure S1). We found that KHC-mCit was diffusely distributed in neuronal processes unless milton was also present, in which case it became highly concentrated on mitochondria (Figure 1C). Thus, milton in neurons can also serve as an adaptor protein for the recruitment of KHC to mitochondria. In the absence of milton, Miro is inadequate to recruit KHC to the mitochondria in either neurons (Figure 1C) or COS cells (Figure S2). This model implies that there is no direct interaction between KHC and Miro. We confirmed this model by immunoprecipitation of tagged KHC and Miro from transfected HEK cells. Immunoprecipitation of KHC efficiently precipitated Miro only if milton was co-expressed (Figure 1D). On longer exposures, low levels of Miro-KHC association were sometimes seen without milton coexpression; these low levels of association were probably mediated by endogenous milton. Thus milton appears to be essential for connecting KHC to Miro on the mitochondrial surface.

Cytosolic Ca^{++} Regulates Mitochondrial Motility in Hippocampal Axons

In order to study the regulation of mitochondrial motility by Ca^{++} and the KHC/milton/Miro complex, mitochondrial movements were examined in cultured rat hippocampal neurons sparsely transfected with RFP-mito. Because axons have a largely uniform microtubule polarity with (+)- ends located distally, we restricted our analysis to axons and identified them by cotransfection with the axonally restricted synaptic vesicle marker, synaptophysin (SYP)-YFP (Chang et al., 2006) (Figure 2A). Axons could also be distinguished from dendrites by their greater length, thin and uniform diameter, sparse branching, and prominent growth cones (Chang et al., 2006). The polarity of an axon was determined by tracing it back to its cell body or forward to its growth cone. Neither significant bleaching nor damage to the mitochondria was observed during 2 hours of imaging. The average velocities of moving mitochondria were: anterograde 0.12±0.01μm/s (n=32 mitochondria), retrograde 0.12±0.01μm/s (n=40). The mitochondria were in anterograde motion 14±2.6% of the time and retrograde 15±2.4% (n=152). The average mitochondrial length was 1.6±0.1μm (n=111) (see Experimental Procedures for analytic methods). These parameters are comparable to previously published values in cultured hippocampal neurons (Overly et al., 1996).

Increasing cytosolic Ca^{++} can reduce mitochondrial movements in many cell types (Chang et al., 2006; Yi et al., 2004), a phenomenon that is independent of mitochondrial membrane potential (Yi et al., 2004). To determine if hippocampal mitochondria were similarly regulated, we increased global intracellular Ca^{++} by applying the calcium ionophore calcimycin (10 μM)

in a saline containing 1.8 mM Ca^{++}. Within 5 minutes of calcimycin addition to the cultures, an obvious decrease of mitochondrial motility (Figure 2B, Movie S1, Table S1), but not synaptic vesicular motility (visualized with SYP-YFP, Figure S3, Table S2), could be observed.

Disruption of the EF Hands in Miro Prevents the Ca^{++}-induced Arrest of Axonal Mitochondria

To determine whether the EF-hands in this motor/adaptor complex mediate the Ca^{++}-dependent regulation of mitochondrial transport, we compared wildtype Miro to a mutated version ($Miro^{KK}$) in which the EF-hands have been disrupted by changing essential glutamates in the Ca^{++}-binding sequence to lysines (Fransson et al., 2006). Each construct was cotransfected with RFP-mito in rat hippocampal neurons and the axonal transport of mitochondria was examined. The location and morphology of axonal mitochondria were grossly normal in both cases when compared to control cultures only expressing RFP-mito (compare Figures 2 and 3). In this regard, neuronal expression differed from what we and others have observed in COS cells where overexpression of either Miro construct caused perinuclear accumulations of mitochondria (Fransson et al., 2006; data not shown). The fraction of time axonal mitochondria were in motion was not significantly different for either construct when compared to cells without transfected Miro, for either anterograde (12±2.4% Miro, n=145 and 17±2.8% $Miro^{KK}$, n=156) or retrograde (14±2.6% Miro, n=145 and 13±2.6% $Miro^{KK}$, n=156) movements. Similarly, their average velocities, lengths, and frequencies of stopping or reversing directions were unaltered by the expression of either wildtype Miro or $Miro^{KK}$ (Table S1, Figure S4).

Addition of calcimycin to raise cytosolic Ca^{++} reduced bidirectional axonal transport of mitochondria in Miro-overexpressing cells, but mitochondria remained highly motile in $Miro^{KK}$-expressing cells (Figure 3, Movies S2, S3). Notably, movement persisted in both the anterograde (presumably kinesin-mediated) and retrograde (presumably dynein-mediated) directions (see Discussion). We analyzed the movement parameters before and after the increase of Ca^{++}, comparing control neurons to those expressing either wildtype Miro or $Miro^{KK}$. We did not observe any significant change in the length of mitochondria upon the addition of calcimycin within the time window for which mitochondrial movements were analyzed (Figure S4A, Table S1), suggesting that the mitochondria we analyzed were morphologically healthy and had not undergone swelling or abnormal fission-and-fusion. The velocities of mitochondria moving in either direction were not significantly different between Miro and $Miro^{KK}$-overexpressing axons, neither before nor after the increase of cytosolic Ca^{++} (Figure S4B, Table S1). However, the percent of time mitochondria move was significantly decreased in axons expressing Miro but not $Miro^{KK}$ after the increase of cytosolic Ca^{++} (Figure 3C, Table S1). Thus, although the basic characteristics of mitochondrial dynamics were unaltered by those mutations, the Ca^{++}-dependent regulation of that motility was prevented by disrupting the EF-hands of Miro.

Ca^{++} Does Not Disrupt the Association of KHC with the milton/Miro Complex or Mitochondria

Because anterograde, microtubule-based motility of mitochondria depends on their attachment to KHC via the adaptor complex containing milton and Miro, we hypothesized that Ca^{++}-binding to Miro might arrest movement by dissociating the complex and thereby releasing mitochondria from their motor. To test this hypothesis, we co-transfected neurons with mCit-tagged KHC and milton, in addition to Miro or $Miro^{KK}$. KHC-mCit was localized to mitochondria both before and after calcimycin addition, in both Miro/milton/KHC and $Miro^{KK}$/milton/KHC transfected axons (Figure 4A, B). The fluorescent intensities of KHC-mCit on mitochondria were not significantly changed after calcimycin addition (Figure 4C). Thus there was no indication that increased cytosolic Ca^{++} released KHC from the mitochondria. We compared the movement of KHC-mCit and RFP-mito, both before and after calcimycin addition and found that KHC-mCit puncta always moved together with RFP-mito

regardless of the direction of movement and was also colocalized with stationary mitochondria. They remained associated with mitochondria before and after calcimycin addition and in both wildtype and mutated Miro (Figures 4D-F, S4A-B, Table S1, Movies S4, S5). The invariant association of KHC with mitochondria indicates that neither the Ca^{++}-dependency of movement nor the choice of anterograde vs. retrograde movement is governed by the association and dissociation of this motor. These physiological observations were also supported by a biochemical analysis of the KHC/milton/Miro complex. High Ca^{++} did not prevent the three components (milton, Miro and KHC) from coprecipitating when coexpressed in HEK cells (Figure 4G). In a further test of the Ca^{++}-dependence of KHC association with mitochondria, we prepared a mitochondrial fraction from rat hippocampal neurons and determined the level of KHC present after washing with either 0 or 2mM Ca^{++}. High Ca^{++} did not dissociate KHC from the mitochondria (Figure 4H).

Ca^{++} Binding to Miro Interferes with KHC Binding to Microtubules

Because the motor/adaptor complex was not disrupted by elevated Ca^{++} and KHC remained associated with mitochondria, we hypothesized that the Ca^{++} might instead regulate via Miro the ability of KHC to interact with microtubules. To test this hypothesis, we performed microtubule cosedimentation experiments. HEK cells transfected with KHC alone, or cotransfected with milton and Miro, were lysed and incubated with polymerized microtubules in either 0 or 2 mM Ca^{++} buffer. The microtubules and any bound proteins were pelleted through a sucrose cushion. When KHC was present without cotransfected milton and Miro, it was exclusively found in the microtubule pellet, whether or not Ca^{++} was present (Figure 5). When KHC was coexpressed with milton and Miro, however, Ca^{++} caused a substantial shift of KHC, together with its adaptor proteins milton and Miro, to the soluble fraction. This shift was observed only when wildtype Miro was expressed; when KHC was coexpressed with the EF-hand-disrupted $Miro^{KK}$ mutant, KHC remained in the microtubule pellet, even in 2 mM Ca^{++}. Thus Ca^{++}, via the EF-hands of Miro, can cause KHC to dissociate from microtubules.

Ca^{++}-dependent Binding of Miro to the N-terminal Motor Domain of KHC

Heretofore, the only interaction observed between Miro and KHC was mediated by milton, which binds to the C-terminus of KHC (Figure 1A) (Glater et al., 2006), whereas the N-terminus of KHC interacts with microtubules. How then do the EF hands of Miro regulate the interaction of KHC with microtubules? We investigated the possibility that Ca^{++} induced a direct interaction of Miro and KHC, and found that Miro and KHC would indeed co-precipitate in elevated Ca^{++} even in the absence of cotransfected milton (Figure 6A-C), although in Ca^{++}-free conditions milton was required. This Ca^{++}-dependent interaction was mediated by the EF hands of Miro; $Miro^{KK}$ did not substantially coprecipitate with KHC in either the presence or absence of Ca^{++} unless milton was present (Figure 6A-C).

To test if the Ca^{++}-dependent coprecipitation of Miro and KHC was a direct interaction or mediated by endogenous milton, and to map the region of interaction, we used truncated KHC (Figure 6D-F). KHC(1-682) lacks the milton-binding site (810-891 of the KHC tail (Glater et al., 2006)). MiroΔTM deletes mitochondrial anchoring the domain (TM, transmembrane domain) of Miro (Glater et al., 2006). The truncated KHC bound MiroΔTM in a Ca^{++}-dependent way, and these interactions were prevented by mutation of the EF hands (Figure 6D-F). These data indicate that the association of KHC and Miro is not dependent on the milton-binding domain of KHC or on a mitochondrial localization for Miro. Indeed, when a construct encoding only the N-terminal motor domain of KHC was coexpressed with Miro they exhibited Ca^{++}-dependent coprecipitation (Figure 6G-H). Thus, Miro interacts with KHC in two ways: the tail of KHC is linked to Miro by milton in a Ca^{++}-independent manner and the motor domain can interact directly with Miro in the presence of Ca^{++}.

The KHC Motor Domain Bound to Miro Does Not Bind to Microtubules

The ability of Miro to bind the motor domain in the presence of Ca^{++} suggested that a direct competition between Miro and microtubules might explain the regulation of anterograde transport by Ca^{++}: the interaction of Miro with the motor domain could cause that domain to dissociate from microtubules. We transfected a truncated KHC containing only the motor domain into HEK cells, together with Miro or $Miro^{KK}$, and performed microtubule cosedimentation experiments as above. Consistently, using Miro-transfected cell lysates, high Ca^{++} shifted the motor domain from the microtubule pellet to the supernatant. This shift was not observed with $Miro^{KK}$-transfected cell lysates (Figure 6I, J). Thus, in a manner mediated by the EF-hands, Ca^{++}-induced binding of Miro to the KHC motor domain, prevents the motor domain from binding to microtubules.

The Switching of the KHC Motor Between Miro- and Microtubule-bound States is Ca^{++}-Concentration Dependent

We determined the range of Ca^{++} concentrations over which Miro could influence the microtubule binding of the motor domain. Microtubule cosedimentations, as described above, were conducted in a series of Ca^{++} concentrations ranging from 0 to 2 mM. The amount of the motor domain bound to microtubules decreased in a concentration-dependent manner, with a 50% reduction in binding occurring in 50 μM free Ca^{++} (Figure 6K, M). The Ca^{++}-dependent binding of the motor domain to Miro showed a reciprocal concentration-dependence, with 50% of maximal binding also occurring in 50 μM free Ca^{++} (Figure 6L, M). The similarity of the concentration-dependences is consistent with a model in which Ca^{++} binding to the EF hands permits Miro to interact with the motor domain and thereby inhibits the binding of KHC to microtubules. This inhibition can account for the Ca^{++}-dependent arrest of anterograde movement of mitochondria, despite the continued association of KHC with the organelle. One prediction of this model is that overexpression of the KHC motor domain alone might compete with endogenous KHC for binding to Miro and thereby interfere with the Ca^{++}-induced arrest of mitochondrial motility. Overexpression of the motor domain had little effect on the properties of mitochondrial movement in axons prior to calcimycin but did indeed prevent Ca^{++}-dependent arrest of mitochondria (Figure S4C, D, Table S3). This observation is consistent with a required interaction of the endogenous motor domain and Miro for disengaging KHC from microtubules.

The EF-hands of Miro Mediate Glutamatergic Regulation of Mitochondrial Motility and are Protective during Excitotoxic Stresses

Glutamatergic synaptic transmission causes Ca^{++} influx in dendrites and the application of glutamate has been shown to arrest dendritic mitochondria in a Ca^{++}-dependent maner (Chang et al., 2006; Li et al., 2004). Therefore, to determine whether a physiologically relevant response to a Ca^{++} signal was mediated by the same mechanism as the calcimycin response, we examined the effects of glutamate application to dendrites of $Miro^{KK}$—expressing neurons. Whereas the percentage of time mitochondria were motion was significantly decreased by glutamate in dendrites expressing Miro, no such inhibition of movement was observed when $Miro^{KK}$ was expressed (Figure 7A-B, Table S4). As observed in axons (Figs, 3 and 4), both anterograde and retrograde movements became Ca^{++} resistant in the presence of $Miro^{KK}$.

In considering the physiological significance of this Ca^{++} effect, we hypothesized that regulation via Miro permits mitochondria to concentrate in sites of high energy demand, where cytosolic Ca^{++} is elevated and in regions where mitochondrial buffering of Ca^{++} is required. This hypothesis predicts that $Miro^{KK}$-transfected neurons would be more susceptible to glutamate excitotoxicity because they would not redistribute mitochondria appropriately. To test this hypothesis, we applied the glutamate-receptor agonist and excitotoxin, NMDA (N-methyl-D-aspartic acid) to Miro or $Miro^{KK}$-transfected neurons for 5 minutes. Transfected

neurons were identified by coexpression of GFP and the concentration/sensitivity of the survival of GFP-expressing neurons was examined 24 h after NMDA incubation. In the absence of NMDA, counts of GFP-alone, GFP/Miro, and GFP/Miro^{KK}-transfected neurons were similar at 24 h and GFP/Miro^{KK} cultures remained healthy for several weeks. Exposure to 3, 10, or 30 μM NMDA reduced the numbers of surviving neurons in all conditions, but survival of GFP/Miro^{KK} neurons was significantly worse than those expressing GFP alone or GFP and Miro. At 30μM NMDA application, approximately 40% of GFP-alone and GFP/Miro-transfected neurons survived, but only 20% of GFP/Miro^{KK}-transfected neurons (Figure 7 C-D). Thus, the ability of the EF-hands of Miro to respond to Ca^{++} protects neurons during excitotoxic challenge.

DISCUSSION

Kinesin motors drive the movements of chromosomes during mitosis and of proteins and organelles in postmitotic cells To accomplish these tasks, their activities must be carefully regulated and recent work has begun to reveal the diversity of mechanisms that orchestrate the kinesins, either through regulation of motor activity or cargo association (Adio et al., 2006; Cai et al., 2007). In addressing how Ca^{++} regulates kinesin-1 in the context of mitochondrial motility, we have determined 1) that the EF-hands of Miro are essential for the Ca^{++}-dependent arrest of axonal mitochondria, whether induced by calcimycin or glutamate, but did not noticeably alter any other aspect of their movements; 2) that kinesin heavy chain remains on mitochondria regardless of whether they are moving or stationary, whether they are moving to (+) or (-) ends, or whether Ca^{++} is at resting or elevated levels; 3) that Ca^{++}, via interaction with Miro, causes the kinesin heavy chain to lose its association with microtubules; 4) that this dissociation arises from the Ca^{++}-dependent binding of the motor domain to Miro; 5) that the EF-hands of Miro mediate the arrest of retrograde as well as anterograde movement of mitochondria; and 6) that this effect enhances neuronal survival under conditions of excitotoxic stress.

The regulation of mitochondrial kinesin-1 can be viewed as a switch between two states of the motor adaptor complex (Figure 7E). In the “on” state, KHC is bound to the mitochondrion by the interaction of its C-terminal tail with milton, which is in turn bound to Miro on the mitochondrial surface. This conformation leaves the N-terminal motor domain of KHC free to interact with microtubules and accomplish anterograde movement. In the “off” state, an additional, direct interaction occurs between the motor domain of KHC and Miro that prevents interactions with microtubules. In other EF-hand proteins, Ca^{++} binding induces a major conformational change (Nelson and Chazin, 1998), and we presume that a similar change in the structure of Miro drives the switch between the “on” and “off” states of the complex. The interaction of the KHC motor domain with Miro may inhibit microtubule binding either by steric interference with the microtubule binding site or by an allosteric change in the structure of the motor domain.

This regulatory mechanism is distinct from those that have previously been described for kinesin-1 in other contexts. The binding of kinesin light chains to the tail domain, for example, can induce a closed, inactive state and cargo-binding can relieve that inhibition (Cai et al., 2007; Reed et al., 2006). However, at least in *Drosophila*, mitochondrial transport in axons is independent of the light chain and the light chain is not present in the KHC/milton/Miro complex (Glater et al., 2006). Moreover, we found no evidence for a change in cargo association: mitochondria retained KHC under all the conditions studied (Figures 4, 6). Although the kinesin regulation reported here is unlike any previously described for a kinesin-1 or indeed any animal kinesin, it may bear some resemblance to the interactions of the Kinesin-like Calmodulin Binding Protein (KCBP) of plants, an unusual minus-end directed motor. The motor region of KCBP can bind either calmodulin or a related protein, KIC, via their EF hands

and in a Ca^{++}-dependent manner (Vinogradova et al., 2004). This binding reaction releases the motor from the microtubule pellet to the supernatant in microtubule-binding assays (Deavours et al., 1998). The EF hands of Miro may similarly bind directly to the motor domain of KHC and interfere with microtubule binding by a comparable mechanism. In a broader sense, the regulation of KHC by Miro also resembles myosin V regulation by calmodulin (Homma et al., 2000).

The complex regulation of mitochondrial distribution is likely to reflect the diverse functions of mitochondria in signaling and energy supply. Ca^{++}-dependent arrest of mitochondrial motility is observed in many cell types, and likely represents a means to two distinct ends: the positioning of mitochondria where they are most needed for Ca^{++}-buffering and the recruitment of mitochondria to cellular regions with insufficient ATP supply. Where ATP is low, Ca^{++}-transport mechanisms are compromised and cytosolic Ca^{++} increases (Yang and Steele, 2000). If randomly moving mitochondria stop where Ca^{++} is elevated, they will be recruited to regions of insufficient ATP and retained there until ATP levels are restored. This mechanism may therefore assist in balancing the distribution of mitochondria throughout the cell. Failure of this mechanism may account for the increased excitotoxicity of NMDA to $Miro^{KK}$-expressing neurons.

An unanticipated finding in the present study was that the EF hands of Miro mediate Ca^{++}-dependent arrest of retrograde motion as well as anterograde (Figures 3, 4). Retrograde motion of axonal mitochondria is dependent on dynein rather than kinesin (Hollenbeck and Saxton, 2005;Pilling et al., 2006). This raises the likelihood that Miro has interactions with the dynein complex in addition to its known interactions with kinesin. At present, little is known about how kinesin and dynein motors interact and whether, or how, they are coordinated (Gross et al., 2007). Estimates of the motor molecules per mitochondrion vary from 2 to 200 (Gross et al., 2007), and it is unknown whether these motors are activated and inactivated in concert. With fluorescent tags on both KHC and mitochondria we have shown that KHC remains associated with mitochondria even when they are moving in the retrograde direction (Figure 4). These kinesin molecules must either be switched off or actively oppose the retrograde movement (Gross et al., 2007). The possibility of a shared association with Miro, therefore, may provide an entry to understanding how opposing motors may be coordinately regulated.

The regulation of mitochondrial dynamics is likely to be extremely intricate, extending well beyond the Ca^{++}-dependent effects on kinesin activity described here. The atypical GTPase-domains in Miro (Fransson et al., 2003; Fransson et al., 2006) and splicing variants of milton (Cox and Spradling, 2006; Glater et al., 2006; Smith et al., 2006) represent additional likely control points. The potential interplay of the GTPase motifs and EF-hands is not presently understood, but may resemble the influence of Ca^{++} on Rho-GTPase in controlling actin dynamics (Aspenstrom et al., 2004; Bader et al., 2004). The splice variants of milton differ in their association with KHC (Glater et al., 2006) and may have tissue specific roles (Cox and Spradling, 2006). In addition, the motility of mitochondria is likely to be interrelated with the fission-fusion machinery, as the dynamin-like GTPase, Drp1, influences mitochondrial density in dendrites (Li et al., 2004), and the absence of fission prevents axonal transport of mitochondria (Verstreken et al., 2005). The Miro homolog of yeast, GEM1p, controls mitochondrial distribution in that organism in a kinesin-independent manner (Frederick et al., 2004) and these additional functions of Miro may be present in higher eukaryotic cells as well (Fransson et al., 2006; Guo et al., 2005). One of the most intriguing potential regulations may be mediated by the enzyme O-GlcNAc transferase (OGT). OGT has been shown to bind to milton and glycosylate it in both mammals (Iyer and Hart, 2003) and *Drosophila* (Glater et al., 2006). Elsewhere, OGT activity has been shown to reflect glucose concentrations and the metabolic state of the cell (Murrey and Hsieh-Wilson, 2008), opening the possibility that the interactions of milton and OGT may permit mitochondrial distribution to be tailored by the

availability of substrates for glycolysis and ATP production. Thus the motor/adaptor complex discussed here may be the nexus of multiple control pathways in addition to the Ca^{++}-sensing role of Miro and is likely to transduce information about local energy supply and demand. These converging signaling pathways will likely regulate mitochondrial dynamics to achieve the most efficient supply and use of energy by the cell.

EXPERIMENTAL PROCEDURES

Constructs

The following constructs were used: pLPS-RFP-mito (Colwill et al., 2006), (No. 11702, Addgene, Cambridge, MA); human Miro, pRK5Myc-Miro1 and pRK5Myc-Miro1E208K,E328K ($Miro^{KK}$), (Fransson et al., 2006); *Drosophila* milton, pCMV-milton A (Stowers et al., 2002); rat KHC, KHC-Myc, KHC1-682-Myc, (Verhey et al., 1998),KHC-ECFP and KHC-mCit (Cai et al., 2007); pCMV-GFP (gift of Dr. Z. Wills); Synaptophysin-YFP, PSD95-YFP (Chang et al., 2006); human KIF5C1-335-EYFP (Smith et al., 2006); and *Drosophila* Miro, pA1T7-DMiroΔTM (Glater et al., 2006). pA1T7-DMiroE234K,E354K,ΔTM($DMiro^{KK}$ΔTM) was QuickChange (Stratagene, La Jolla, CA) to introduce into *Drosophila* Miro the mutations equivalent to E208K and E328K in human Miro.

Cell Culture

Rat hippocampal cells were dissected and dissociated from day 18 embryos, cultured for 8-11 days, transfected with Lipofectamine 2000 (Invitrogen), and imaged 2-4 days later. COS and HEK293T cells were transfected with calcium phosphate. Even when four constructs were simultaneously transfected into neurons or HEK cells, the extent of coexpression was greater than 95%, as determined by retrospective immunostaining (Supplementary Data and Figure S5).

Immunostaining and Confocal Microscopy

Immunocytochemistry was performed as previously described (Glater et al., 2006; Stowers et al., 2002) with mouse anti-Myc (9E10, Santa Cruz Biotechnology, Inc., Santa Cruz, CA) at 1:300 and Cy5-conjugated anti-mouse IgG (Jackson ImmunoResearch Laboratories, West Grove, PA) at 1:500. MitoTracker Orange (Invitrogen) was applied at 100 nM for 10 min. Cells were imaged at room temperature (20°C) with a 63×/NA1.4 oil Plan-Apochromat objective on a laser scanning confocal microscope (LSM 510 META/NLO; Carl Zeiss MicroImaging, Inc., Thornwood, NY) with LSM software 3.2 (Carl Zeiss MicroImaging, Inc.). Images were processed with Photoshop 10.0 (Adobe, San Jose, CA) using only linear adjustments of contrast and color, and Illustrator 13.0 (Adobe).

Live Image Acquisition and Quantification

Confocal images (see Supplemental Data) were captured every 5-10 seconds before and after calcimycin treatments. 60-150 μm of axon at least 250 μm away from the cell body was selected for analysis. For glutamate stimulation, 30-110 μm of dendrite was selected for analysis. Kymographs were generated (Metamorph software, MDC, CA), that represented an interval of 100 s taken before the application of calcimycin or glutamate and 5 min after calcimycin or 1 min after glutamate addition. Each kymograph was then imported into a macro written in Labview (NI, TX), and individual RFP-mito or SYP-YFP puncta were traced using a mouse-driven cursor at the center of the RFP-mito or SYP-YFP object. By using Matlab (The MathWorks, MA), we determined the following parameters: 1) the instantaneous velocity of each mitochondrion, 2) the average velocity of those mitochondria that were in motion, 3) the percent of time each mitochondrion was in motion, 4) stop frequency, and 5) turn back frequency. The lengths of mitochondria were also measured 100 s before and after the 5-min

calcimycin exposure. A threshold velocity was defined as 0.05μm/s which was equivalent to a displacement of 1 pixel over a time lapse of 1 pixel and exceeded the bias caused by recording drift and mouse-positioning (see Supplemental Data). Velocities less than 0.05μm/s were considered zero.

Coimmunoprecipitation and Microtubule Cosedimentation

HEK cells were lysed in buffer as in Glater et al., 2006, but with EDTA replaced by 5mM EGTA and 0 Ca^{++}, or by 2 mM Ca^{++}, or by a series of low Ca^{++} conditions (Figure 6K,L) for which the free Ca^{++} concentration had been calculated (Maxchelator; http://www.stanford.edu/~cpatton/maxc.html). Coimmunoprecipitations were performed as described in Glater et al., 2006. Lysates were incubated with rabbit anti-GFP (Invitrogen), mouse anti-Myc (9E10, Santa Cruz Biotechnology, Inc.), or rabbit anti-hMiro1 (Fransson et al., 2003), and protein A-Sepharose beads (GE Healthcare, Piscataway, NJ) for 2-3 hours at 4°C. Immunoprecipitates were analyzed by SDS-PAGE and immunoblotted as indicated (See Supplemental Data)

For cosedimentation experiments, polymerized microtubules were prepared by incubating tubulin (Cytoskeleton Inc., CO) with 1mM GTP and 100 μM Taxol (Sigma, MO) at 37 °C 1 hour. Cell lysates were then incubated with 20 mM Taxol and 0.1 mg/ml polymerized microtubules for 30 minutes at room temperature without ATP. The microtubule pellet and bound proteins were collected by centrifugation at 21,000g for 30 minutes through a 10% sucrose cushion. Soluble proteins in the supernatant were TCA precipitated and both supernatant and microtubules pellet were analyzed by SDS-PAGE and immunoblotted as indicated (see Supplemental Data).

For quantitative immunoprobing, blots were probed with anti-GFP (Invitrogen) and Cy5 goat anti-rabbit (GE Healthcare) at 1:5000 and scanned by Typhoon Trio Imaging Scanner (Amersham BioSciences, Piscataway, NJ). Fluorescent intensity of the bands was quantitated by fluorescence detection in the linear range. The intensity of each KIF5C(1-335)-YFP band was normalized to an unrelated control IgG band on the same blot.

Preparation of Mitochondrial Fractions

Mitochondria were prepared from cultured rat hippocampal neurons by differential centrifugation (see Supplemental Data). The mitochondrial pellet was resuspended in either 0 or 2 mM Ca^{++} isolation buffer, and centrifuged again. The supernatant (wash) and the mitochondrial pellet were collected separately. 3.5% of the non-mitochondrial fraction, 10% of mitochondrial fraction, and 10% of wash were then loaded in SDS-PAGE and analyzed by Western Blotting with mouse anti-KHC (H2) at 1:400, rabbit anti-VDAC at 1:1000 (Bioreagents, Golden, CO), and mouse anti-synaptophysin at 1:200 (gift of Dr. F. Sun).

Statistical Analysis

Throughout the paper, the distribution of data points is expressed as mean ± standard error of the mean. The Mann-Whitney *U* tests were used for statistical analysis unless otherwise indicated.

Supplementary Material

Refer to Web version on PubMed Central for supplementary material.

Acknowledgments

We thank I. Rappley, Drs. F. Sun, Z. Wills, P. Aspenström, K. J. Verhey, A. M. Craig, T. Pawson, G. W. Hart, and F. A. Stephenson for reagents; S. Vasquez, Drs. Z. Wills, M. Greenberg, and Z. He for assistance with hippocampal cultures, Dr. L. Bu and the Developmental Disorders Research Center Imaging Core and E. Pogoda for technical assistance; Dr. Y. Chu for assistance with Matlab script and a Labview macro. This work was supported by NIH RO1GM069808.

REFERENCES

Adio S, Reth J, Bathe F, Woehlke G. Regulation mechanisms of Kinesin-1. J Muscle Res Cell Motil 2006;27:153–160. [PubMed: 16450053]

Aspenstrom P, Fransson A, Saras J. Rho GTPases have diverse effects on the organization of the actin filament system. Biochem J 2004;377:327–337. [PubMed: 14521508]

Bader MF, Doussau F, Chasserot-Golaz S, Vitale N, Gasman S. Coupling actin and membrane dynamics during calcium-regulated exocytosis: a role for Rho and ARF GTPases. Biochim Biophys Acta 2004;1742:37–49. [PubMed: 15590054]

Beck M, Brickley K, Wilkinson HL, Sharma S, Smith M, Chazot PL, Pollard S, Stephenson FA. Identification, molecular cloning, and characterization of a novel GABAA receptor-associated protein, GRIF-1. J Biol Chem 2002;277:30079–30090. [PubMed: 12034717]

Boldogh IR, Pon LA. Mitochondria on the move. Trends Cell Biol 2007;17:502–510. [PubMed: 17804238]

Brady ST, Lasek RJ, Allen RD, Yin HL, Stossel TP. Gelsolin inhibition of fast axonal transport indicates a requirement for actin filaments. Science 1982;310:56–58.

Brickley K, Smith MJ, Beck M, Stephenson FA. GRIF-1 and OIP106, members of a novel gene family of coiled-coil domain proteins: association in vivo and in vitro with kinesin. J Biol Chem 2005;280:14723–14732. [PubMed: 15644324]

Cai D, Hoppe AD, Swanson JA, Verhey KJ. Kinesin-1 structural organization and conformational changes revealed by FRET stoichiometry in live cells. J Cell Biol 2007;176:51–63. [PubMed: 17200416]

Chada SR, Hollenbeck PJ. Mitochondrial movement and positioning in axons: the role of growth factor signaling. J Exp Biol 2003;206:1985–1992. [PubMed: 12756280]

Chada SR, Hollenbeck PJ. Nerve growth factor signaling regulates motility and docking of axonal mitochondria. Curr Biol 2004;14:1272–1276. [PubMed: 15268858]

Chang DT, Honick AS, Reynolds IJ. Mitochondrial trafficking to synapses in cultured primary cortical neurons. J Neurosci 2006;26:7035–7045. [PubMed: 16807333]

Chen H, Chan DC. Critical dependence of neurons on mitochondrial dynamics. Curr Opin Cell Biol 2006;18:453–459. [PubMed: 16781135]

Colwill K, Wells CD, Elder K, Goudreault M, Hersi K, Kulkarni S, Hardy WR, Pawson T, Morin GB. Modification of the Creator recombination system for proteomics applications--improved expression by addition of splice sites. BMC Biotechnol 2006;6:13. [PubMed: 16519801]

Cox RT, Spradling AC. Milton controls the early acquisition of mitochondria by Drosophila oocytes. Development 2006;133:3371–3377. [PubMed: 16887820]

Deavours BE, Reddy AS, Walker RA. Ca2+/calmodulin regulation of the Arabidopsis kinesin-like calmodulin-binding protein. Cell Motil Cytoskeleton 1998;40:408–416. [PubMed: 9712269]

Fransson A, Ruusala A, Aspenstrom P. Atypical Rho GTPases have roles in mitochondrial homeostasis and apoptosis. J Biol Chem 2003;278:6495–6502. [PubMed: 12482879]

Fransson S, Ruusala A, Aspenstrom P. The atypical Rho GTPases Miro-1 and Miro-2 have essential roles in mitochondrial trafficking. Biochem Biophys Res Commun 2006;344:500–510. [PubMed: 16630562]

Frederick RL, McCaffery JM, Cunningham KW, Okamoto K, Shaw JM. Yeast Miro GTPase, Gem1p, regulates mitochondrial morphology via a novel pathway. J Cell Biol 2004;167:87–98. [PubMed: 15479738]

Glater EE, Megeath LJ, Stowers RS, Schwarz TL. Axonal transport of mitochondria requires milton to recruit kinesin heavy chain and is light chain independent. J Cell Biol 2006;173:545–557. [PubMed: 16717129]

Gross SP, Vershinin M, Shubeita GT. Cargo transport: two motors are sometimes better than one. Curr Biol 2007;17:R478–486. [PubMed: 17580082]

Guo X, Macleod GT, Wellington A, Hu F, Panchumarthi S, Schoenfield M, Marin L, Charlton MP, Atwood HL, Zinsmaier KE. The GTPase dMiro is required for axonal transport of mitochondria to Drosophila synapses. Neuron 2005;47:379–393. [PubMed: 16055062]

Hollenbeck PJ, Saxton WM. The axonal transport of mitochondria. J Cell Sci 2005;118:5411–5419. [PubMed: 16306220]

Homma K, Saito J, Ikebe R, Ikebe M. Ca(2+)-dependent regulation of the motor activity of myosin V. J Biol Chem 2000;275:34766–34771. [PubMed: 10945977]

Hurd DD, Saxton WM. Kinesin mutations cause motor neuron disease phenotypes by disrupting fast axonal transport in Drosophila. Genetics 1996;144:1075–1085. [PubMed: 8913751]

Iyer SP, Hart GW. Roles of the tetratricopeptide repeat domain in O-GlcNAc transferase targeting and protein substrate specificity. J Biol Chem 2003;278:24608–24616. [PubMed: 12724313]

Kang JS, Tian JH, Pan PY, Zald P, Li C, Deng C, Sheng ZH. Docking of axonal mitochondria by syntaphilin controls their mobility and affects short-term facilitation. Cell 2008;132:137–148. [PubMed: 18191227]

Li Z, Okamoto K, Hayashi Y, Sheng M. The importance of dendritic mitochondria in the morphogenesis and plasticity of spines and synapses. Cell 2004;119:873–887. [PubMed: 15607982]

Morris RL, Hollenbeck PJ. Axonal transport of mitochondria along microtubules and F-actin in living vertebrate neurons. J Cell Biol 1995;131:1315–1326. [PubMed: 8522592]

Murrey HE, Hsieh-Wilson LC. The Chemical Neurobiology of Carbohydrates. Chem Rev. 2008in press

Nelson MR, Chazin WJ. Structures of EF-hand Ca(2+)-binding proteins: diversity in the organization, packing and response to Ca2+ binding. Biometals 1998;11:297–318. [PubMed: 10191495]

Overly CC, Rieff HI, Hollenbeck PJ. Organelle motility and metabolism in axons vs dendrites of cultured hippocampal neurons. J Cell Sci 1996;109(Pt 5):971–980. [PubMed: 8743944]

Petrozzi L, Ricci G, Giglioli NJ, Siciliano G, Mancuso M. Mitochondria and neurodegeneration. Biosci Rep 2007;27:87–104. [PubMed: 17486441]

Pilling AD, Horiuchi D, Lively CM, Saxton WM. Kinesin-1 and Dynein are the primary motors for fast transport of mitochondria in Drosophila motor axons. Mol Biol Cell 2006;17:2057–2068. [PubMed: 16467387]

Reed NA, Cai D, Blasius TL, Jih GT, Meyhofer E, Gaertig J, Verhey KJ. Microtubule acetylation promotes kinesin-1 binding and transport. Curr Biol 2006;16:2166–2172. [PubMed: 17084703]

Rintoul GL, Filiano AJ, Brocard JB, Kress GJ, Reynolds IJ. Glutamate decreases mitochondrial size and movement in primary forebrain neurons. J Neurosci 2003;23:7881–7888. [PubMed: 12944518]

Smith MJ, Pozo K, Brickley K, Stephenson FA. Mapping the GRIF-1 binding domain of the kinesin, KIF5C, substantiates a role for GRIF-1 as an adaptor protein in the anterograde trafficking of cargoes. J Biol Chem 2006;281:27216–27228. [PubMed: 16835241]

Stowers RS, Megeath LJ, Gorska-Andrzejak J, Meinertzhagen IA, Schwarz TL. Axonal transport of mitochondria to synapses depends on milton, a novel Drosophila protein. Neuron 2002;36:1063–1077. [PubMed: 12495622]

Szabadkai G, Simoni AM, Bianchi K, De Stefani D, Leo S, Wieckowski MR, Rizzuto R. Mitochondrial dynamics and Ca2+ signaling. Biochim Biophys Acta 2006;1763:442–449. [PubMed: 16750865]

Tanaka Y, Kanai Y, Okada Y, Nonaka S, Takeda S, Harada A, Hirokawa N. Targeted disruption of mouse conventional kinesin heavy chain, kif5B, results in abnormal perinuclear clustering of mitochondria. Cell 1998;93:1147–1158. [PubMed: 9657148]

Verhey KJ, Lizotte DL, Abramson T, Barenboim L, Schnapp BJ, Rapoport TA. Light chain-dependent regulation of Kinesin's interaction with microtubules. J Cell Biol 1998;143:1053–1066. [PubMed: 9817761]

Verstreken P, Ly CV, Venken KJ, Koh TW, Zhou Y, Bellen HJ. Synaptic mitochondria are critical for mobilization of reserve pool vesicles at Drosophila neuromuscular junctions. Neuron 2005;47:365–378. [PubMed: 16055061]

Vinogradova MV, Reddy VS, Reddy AS, Sablin EP, Fletterick RJ. Crystal structure of kinesin regulated by Ca(2+)-calmodulin. J Biol Chem 2004;279:23504–23509. [PubMed: 14988396]

Yang Z, Steele DS. Effects of cytosolic ATP on spontaneous and triggered Ca2+-induced Ca2+ release in permeabilised rat ventricular myocytes. J Physiol 2000;523(Pt 1):29–44. [PubMed: 10673543]

Yi M, Weaver D, Hajnoczky G. Control of mitochondrial motility and distribution by the calcium signal: a homeostatic circuit. J Cell Biol 2004;167:661–672. [PubMed: 15545319]

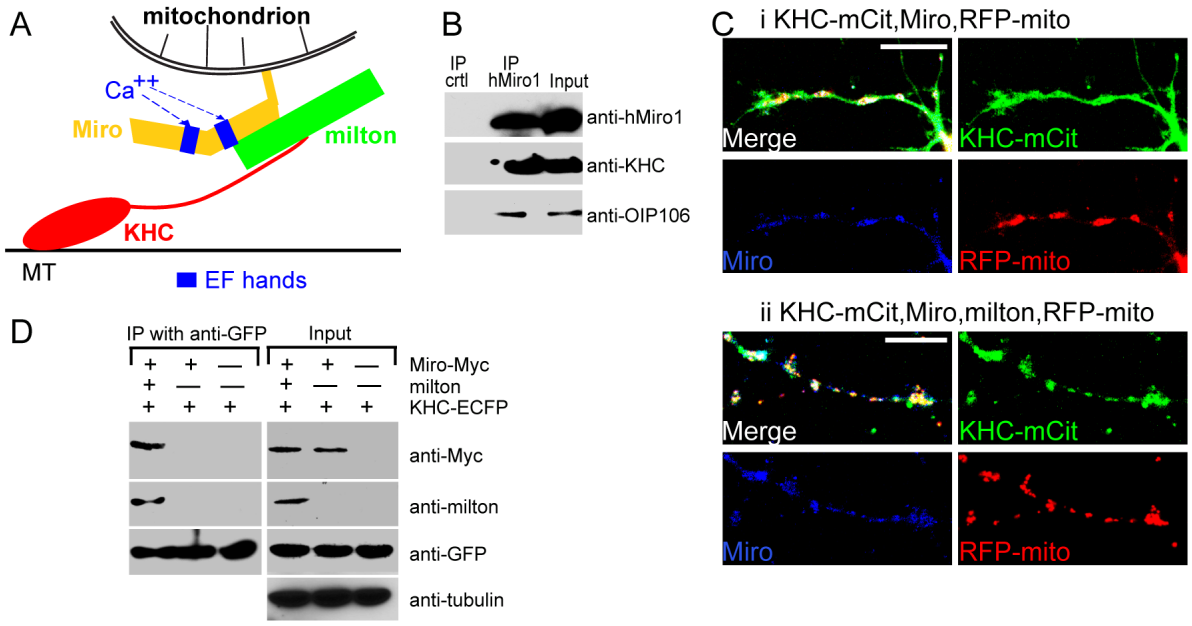

Figure 1. Milton Recruits KHC to Neuronal Mitochondria

(A) Model of the Miro/milton/KHC complex that mediates anterograde transport of mitochondria on microtubules (MT). The EF-hands of Miro are marked in blue. (B) The endogenous motor/adaptor complex from HEK 293T cells was immunoprecipitated with anti-hMiro1 and probed with anti-KHC, anti-hMiro1, and anti-OIP106 (one of two human homologs of milton). Milton, Miro, and KHC were precipitated by anti-hMiro1, but not by a control rabbit IgG. Input lanes were loaded with one fifth the amount of homogenate used for the precipitations. The entire precipitate was loaded in the IP lanes. (C) KHC is localized to mitochondria in the presence (*ii*) but not the absence (*i*) of milton. Neurites of rat hippocampal neurons transfected with KHC-mCit (green), Miro-Myc (blue) and RFP-mito (red). KHC-mCit is diffuse in the absence of milton but mitochondrial when milton is coexpressed. Scale bars, 10 μm. (D) The coimmunoprecipitation of Miro-Myc and KHC-ECFP from HEK cells requires milton. Complexes (IP) were precipitated from cell lysates (Input), in Ca^{++}-free buffer, with anti-GFP. Input lanes contained one fifth the amount of homogenate immunoprecipitated, and were probed with anti-tubulin to control for differences in protein inputs.

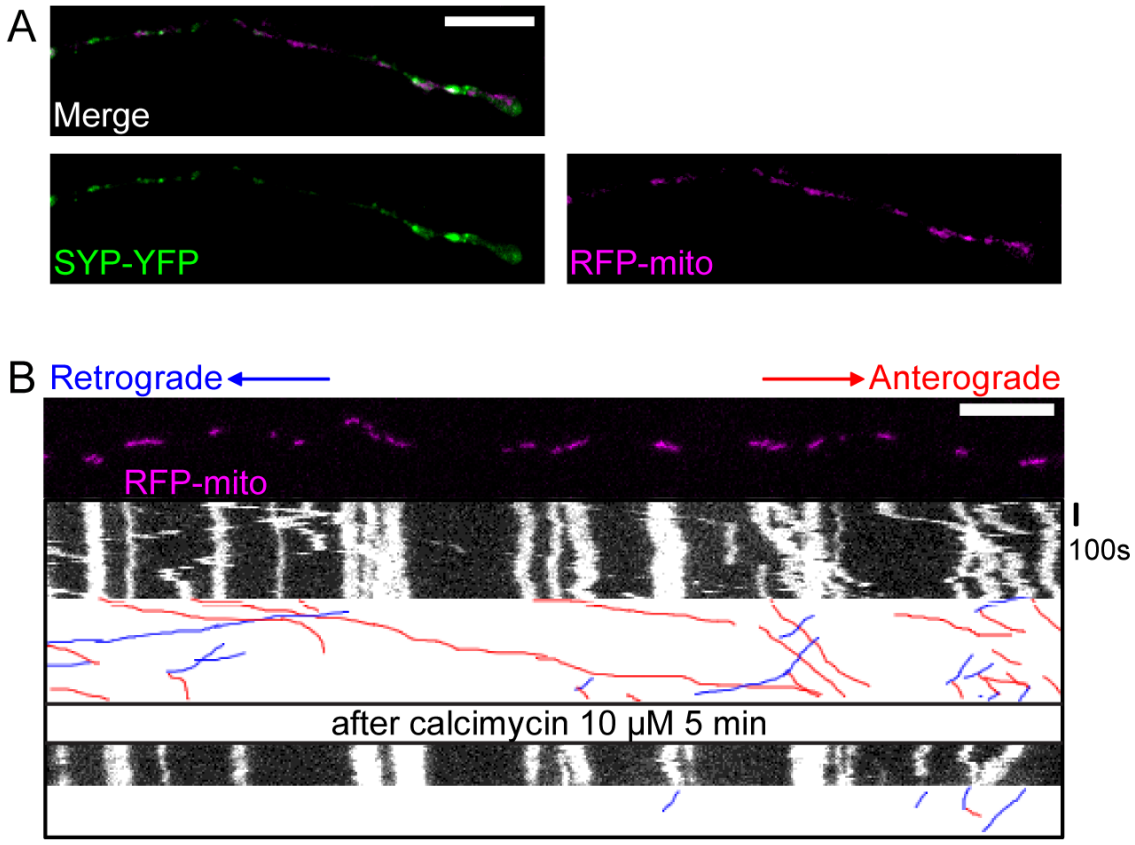

Figure 2. Ca^{++} Influx Inhibits Axonal Transport of Hippocampal Mitochondria

(A) A representative axon of a neuron transfected with the axonal marker synaptophysin-YFP (SYP-YFP, green), and RFP-mito (magenta). (B) Application of calcimycin inhibited mitochondrial movements. The first frame of the live-imaging movie (top panel) and kymographs generated from the movie, in which the *x* axis represents the mitochondrial position and the *y* axis is time. Vertical white lines represent stationary mitochondria and diagonal lines represent moving mitochondria. Below each kymograph are hand-drawn traces of the diagonal lines, in which anterograde movements are red and retrograde blue. Scale bars, 10 μm.

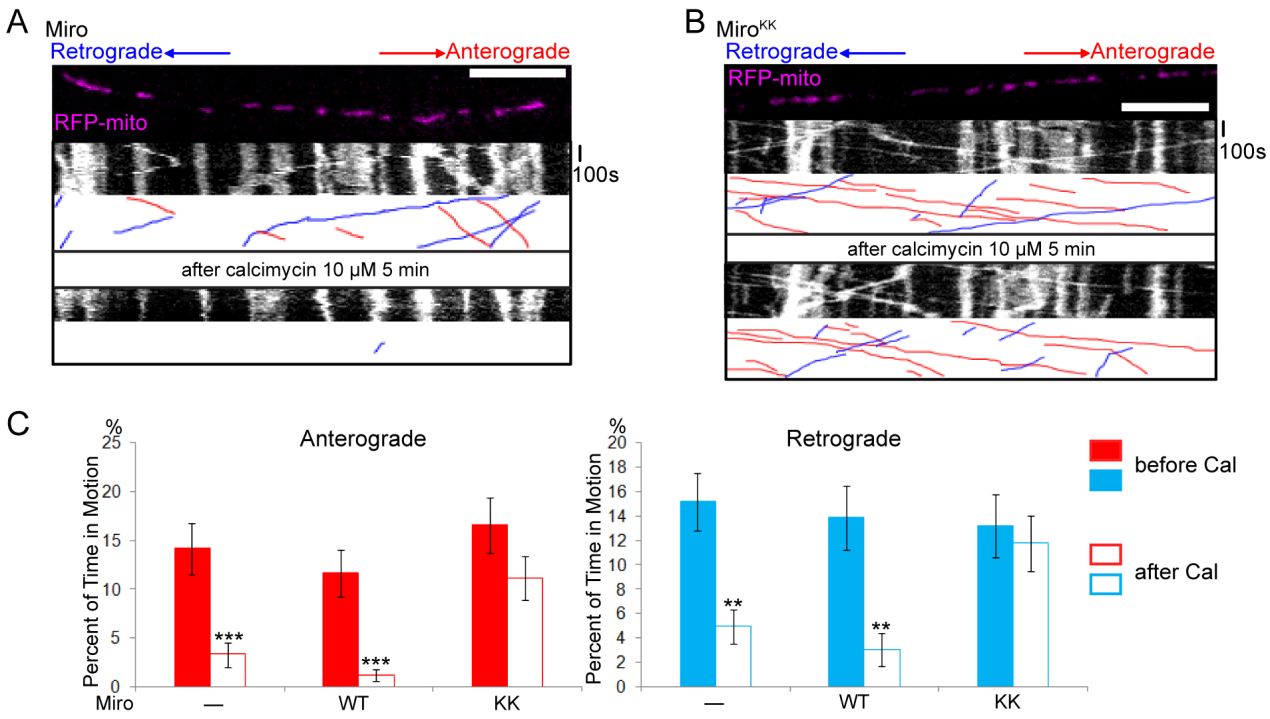

Figure 3. EF-hand Mutations in Miro Prevent the Inhibition by Ca^{++} of Mitochondrial Axonal Transport

(A,B) Mitochondrial motility in the axon of a neuron transfected with SYP-YFP, RFP-mito, and Miro-Myc (A) or $Miro^{KK}$ (B). The first frame and kymograph of mitochondria labeled with RFP-mito are paired with hand-drawn traces that extract those mitochondria moving anterograde (red) or retrograde (blue). Kymographs were made before (upper) and after (lower) 5 minutes in the presence of calcimycin. (C) From kymographs as in A and B, the percent of time each mitochondrion was in motion was determined and averaged (n=145-156 mitochondria from 10 axons and 4 separate transfections per genotype). Calcimycin (Cal) inhibited both directions of movement in control and Miro-transfected, but not $Miro^{KK}$-transfected axons. *, <0.05, **, <0.01, ***, <0.001, and error bars represent mean±S.E.M. here and for all figures. Scale bars, 10 μm.

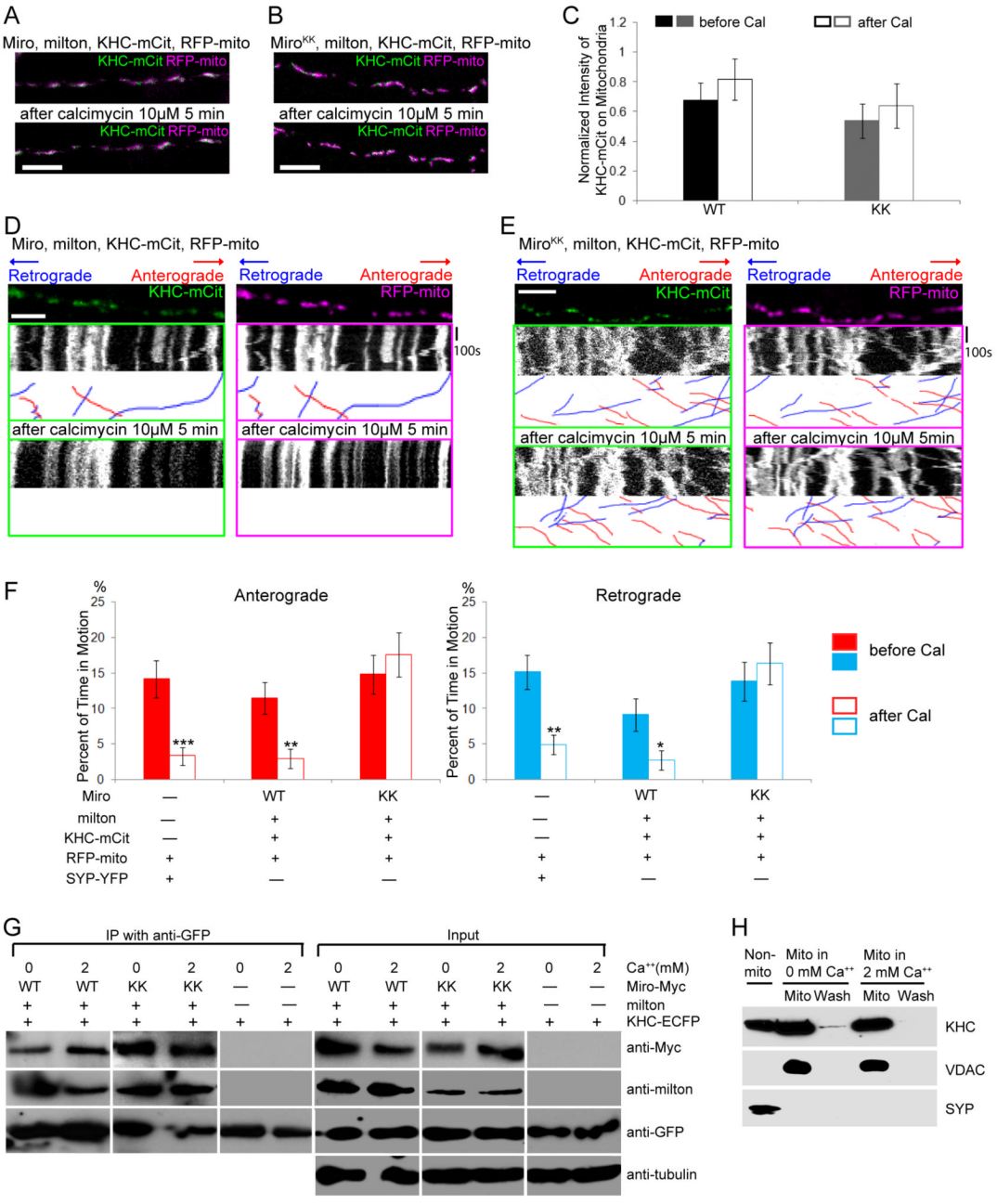

Figure 4. All Axonal Mitochondria Have KHC

(A, B) In axons transfected with KHC-mCit (green), RFP-mito (magenta), milton, and Miro (A) or Miro^{KK} (B), KHC colocalizes with mitochondria both before and after calcimycin addition. (C) Quantification of the fluorescent KHC present on mitochondria defined by the intensity of mCit in the region overlapping RFP-mito, averaged across 30-31 mitochondria from 3 independent transfections, before and after calcimycin (Cal) application. No significant change in intensity was detected upon calcimycin application ($P>0.23$ by Mann-Whitney *U* test). WT, Miro/milton/KHC-transfected neurons; KK, Miro^{KK}/milton/KHC-transfected neurons. (D, E) In kymographs from axons like those in A and B, KHC-mCit and RFP-mito colocalize on stationary mitochondria and move congruently, regardless of the direction of

motion, both before and after calcimycin addition. (F) Significant inhibition of movement by calcimycin (Cal) was found in control and Miro/milton/KHC-transfected but not in $Miro^{KK}$/milton/KHC-transfected neurons. n=144-152 mitochondria from 10 axons and 4 separate transfections. (G) Ca^{++} does not cause dissociation of the milton/Miro/KHC complex. HEK cells were transfected with Miro or $Miro^{KK}$ together with KHC-ECFP and milton, and lysed in either 5mM EGTA or 2mM Ca^{++}. KHC-ECFP was precipitated with anti-GFP and the precipitate (IP) was assayed. Input lanes were loaded with one fifth the amount of homogenate used for immunoprecipitations, and anti-tubulin was used as a loading control. (H) A mitochondrial enriched fraction from cultured rat hippocampal neurons was separated from other cytoplasmic components (Non-mito), and resuspended in either 0 or 2 mM Ca^{++} buffer. After centrifugation the pellet (Mito) and supernatant (Wash) were separated by SDS-PAGE and assayed for endogenous KHC, the mitochondrial marker VDAC, and the synaptic vesicle marker SYP. Scale bars, 10 μm.

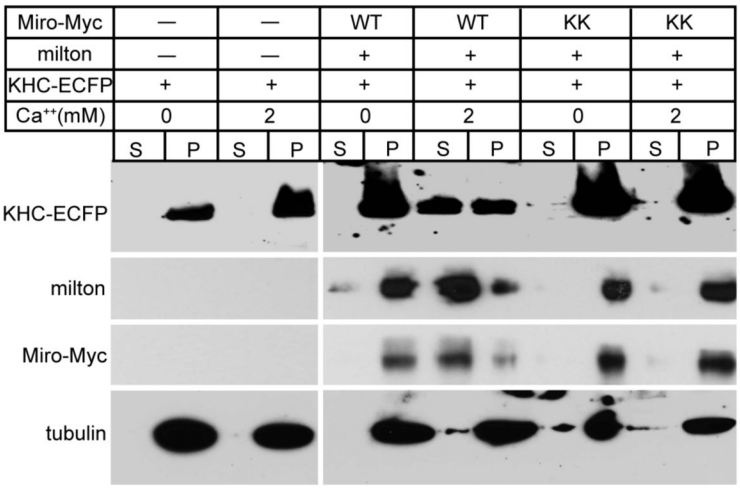

Figure 5. Ca^{++}, via Miro, Releases KHC from Microtubules

Lysates of HEK cells, transfected as indicated, were mixed with Taxol-stabilized microtubules in either 0 or 2 mM Ca^{++} buffer prior to sedimentation of the microtubules and microtubule-bound proteins by centrifugation (pellet, P), leaving unbound proteins in the supernatant fraction (S). Equivalent fractions of the supernatant and pellet were assayed for KHC-ECFP, milton, Miro-Myc, and tubulin.

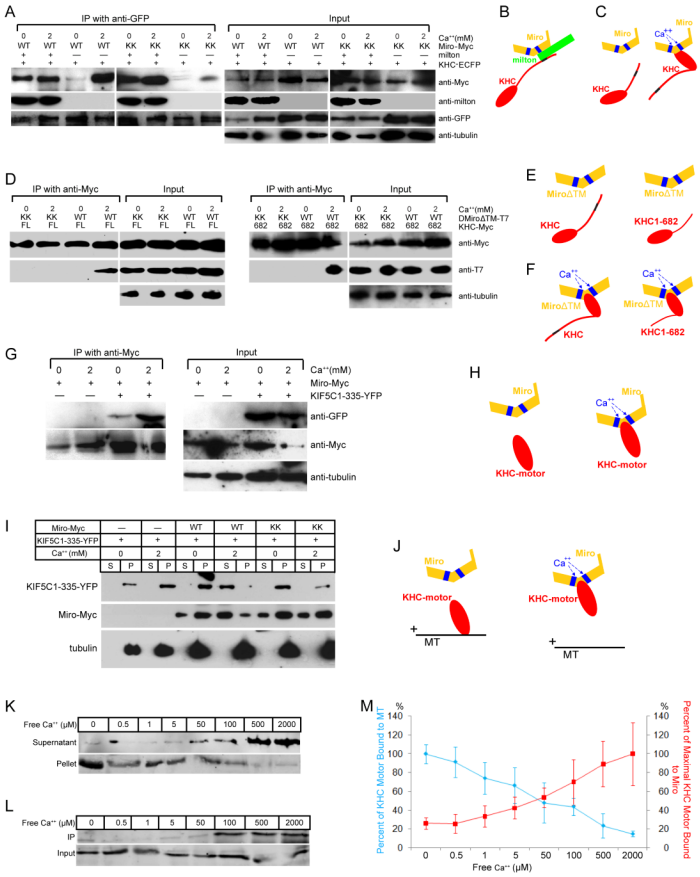

Figure 6. Binding of the Kinesin Motor Domain to Microtubules is Inhibited by Ca^{++}-dependent Interactions with Miro

(A) Immunoprecipitations in the presence or absence of Ca^{++} of KHC-ECFP (with anti-GFP) from lysates of HEK cells, transfected as indicated. In the presence of milton, neither Ca^{++} nor the EF-hands are required for Miro to precipitate with KHC, but in the absence of milton, both are needed (for Ca^{++}, compare third and fourth lanes; for the EF-hands compare fourth and eighth lanes). Low levels of coprecipitation in their absence may be mediated by endogenous milton. (B, C) Illustration of the two modes of association of Miro and KHC, a Ca^{++}-independent association via milton (B) and a Ca^{++}-dependent, milton-independent association (C). Blue boxes represent EF-hands; the black region represents the milton binding site in KHC. (D) Immunoprecipitations with anti-Myc from cells expressing Myc-tagged full length (FL, left two panels) or truncated KHC 1-682 (682, right two panels), and T7-tagged DMiroΔTM, but not milton. (E, F) Illustration of the persistence of the Ca^{++}-induced association of Miro and KHC, despite deletions of the KHC tail and TM domain of Miro. (G) Immunoprecipitations with anti-Myc from cells transfected with Miro-Myc and the kinesin motor domain (YFP-tagged KIF5C1-335). (H) Illustration of the dependence of motor domain/Miro interactions on Ca^{++} and the EF hands of Miro. (I) Microtubule cosedimentations were performed in either 0 or 2 mM Ca^{++} buffer and with Taxol-stabilized microtubules and lysates of the indicated transfected HEK cells. Equal volumes of supernatants (S) and microtubule pellets (P) were loaded and probed separately for KIF5C(1-335)-YFP, Miro-Myc or tubulin. (J) Illustration of the Ca^{++}-dependent, EF-hand-dependent shift of the motor domain from microtubules to Miro, as in (G-I). (K) Ca^{++} dependence of the cosedimentation of the motor domain KIF5C(1-335)-YFP with microtubules, as in (I), in the presence of Miro-Myc, and the indicated free Ca^{++} concentrations. The level of KIF5C(1-335)-YFP in each fraction was determined with anti-

GFP. (L) Ca^{++} dependence of the binding of Miro-Myc to KIF5C(1-335)-YFP, by precipitation from lysates of transfected HEK cells with anti-Myc and probing with anti-GFP (KIF5C (1-335)-YFP). (M) Quantification of Ca^{++} dependence of motor-domain cosedimentation with microtubules (as in K) and coprecipitation with Miro (as in L). The percent bound to microtubules was calculated as the intensity of the band in the pellet divided by the summed intensity of bands in both pellet and supernatant, and was defined as 100% in 0 Ca^{++}. n=3 transfections. The percent of maximal binding to Miro was defined as the intensity of the precipitated band normalized to its input and set at 100% in 2 mM Ca^{++}. n=3 transfections. For each section, input lanes contained one fifth of the amounts used for immunoprecipitation, and anti-tubulin was used as a loading control.

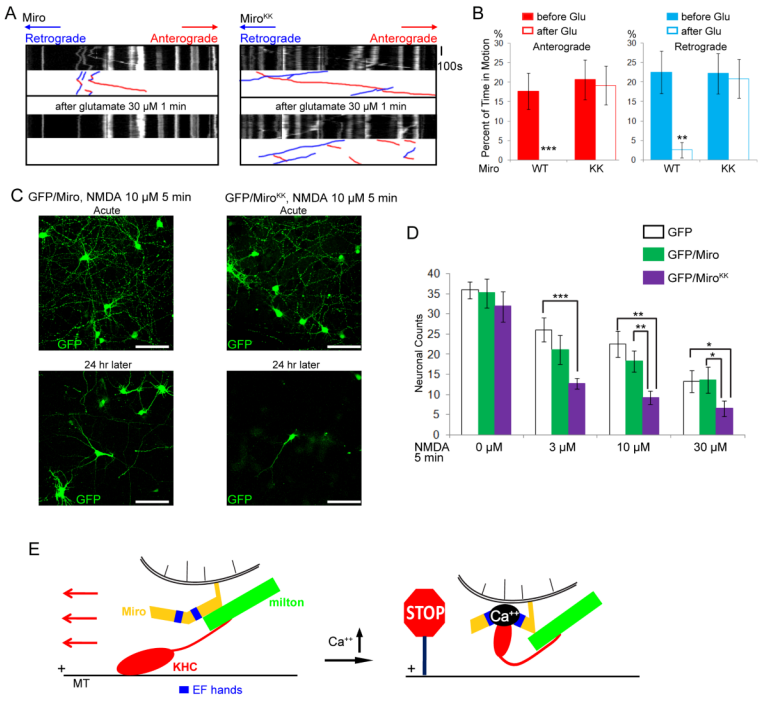

Figure 7. The EF-hands of Miro Mediate Responses of Dendritic Mitochondria to Glutamate and Protect against Excitotoxicity

(A) Mitochondrial motility in dendrites of neurons transfected with Miro-Myc (left panels), or Miro^{KK}-Myc (right panels), together with PSD95-YFP (to mark dendrites), and RFP-mito. Kymographs of RFP-mito were made before (upper) and after (lower) a 1 min exposure to glutamate. (B) From kymographs as in A, the percent of time mitochondria were in motion was determined and averaged (n=53-61 mitochondria from 6 axons and 3 separate transfections). Glutamate (Glu) arrested bidirectional mitochondrial movement in Miro-transfected, but not Miro^{KK}-transfected dendrites. (C) Representative 25× magnification views of neurons transfected with GFP and Miro (left two panels), or GFP and Miro^{KK} (right two panels). After incubation with 10μM NMDA for 5 min, the neurons were either imaged directly (acute) or cultured for 24 h and then imaged. Scale bars, 100 μm. (D) Quantification of surviving neurons. NMDA (0 to 30 μM) was incubated with the transfected neurons for 5 min, and GFP positive neurons were counted 24 h later under 25× along one diameter of the coverslip. Each data point was from 10 coverslips from 3 separate transfections. Significantly different pairs are marked. (E) Schematic model of the means by which Ca^{++} interacts with Miro to regulate the anterograde motility of mitochondria.